Effects of site-specific guanine C8-modifications on an intramolecular DNA G-quadruplex

Christopher Jacques Lech, Joefina Kim Cheow Lim, Jocelyn Mei Wen Lim, Samir Amrane, Brahim Heddi, and Anh Tuân Phan*

School of Physical and Mathematical Sciences,
Nanyang Technological University, Singapore 637371

*Corresponding author: phantuan@ntu.edu.sg

Supporting Information

Full Reference 51

Frisch, M. J.; Trucks, G. W.; Schlegel, H. B.; Scuseria, G. E.; Robb, M. A.; Cheeseman, J. R.; Montgomery, J. A., Jr.; Vreven, T.; Kudin, K. N.; Burant, J. C.; Millam, J. M.; Iyengar, S. S.; Tomasi, J.; Barone, V.; Mennucci, B.; Cossi, M.; Scalmani, G.; Rega, N.; Petersson, G. A.; Nakatsuji, H.; Hada, M.; Ehara, M.; Toyota, K.; Fukuda, R.; Hasegawa, J.; Ishida, M.; Nakajima, T.; Honda, Y.; Kitao, O.; Nakai, H.; Klene, M.; Li, X.; Knox, J. E.; Hratchian, H. P.; Cross, J. B.; Bakken, V.; Adamo, C.; Jaramillo, J.; Gomperts, R. ; Stratmann, R. E.; Yazyev, O.; Austin, A. J.; Cammi, R.; Pomelli, C.; Ochterski, J. W.; Ayala, P. Y.; Morokuma, K.; Voth, G. A.; Salvador, P.; Dannenberg, J. J.; Zakrzewski, V. G.; Dapprich, S.; Daniels, A. D.; Strain, M. C.; Farkas, O.; Malick, D. K.; Rabuck, A. D. ; Raghavachari, K.; Foresman, J. B. ; Ortiz, J. V.; Cui, Q.; Baboul, A. G.; Clifford, S.; Cioslowski, J.; Stefanov, B. B.; Liu, G.; Liashenko, A.; Piskorz, P.; Komaromi, I.; Martin, R. L.; Fox, D. J.; Keith, T.; Al-Laham, M. A.; Peng, C. Y.; Nanayakkara, A.; Challacombe, M.; Gill, P. M. W.; Johnson, B.; Chen, W.; Wong, M. W.; Gonzalez, C.; Pople, J. A.; Gaussian 03, Revision E01; Gaussian, Inc., Wallingford CT, 2004

SUPPLEMENTARY FIGURE LEGENDS

Fig. S1. Monitoring folding topology with CD absorption spectra: A comparison of CD spectra for sequences containing single position substitutions in **(a)** residue 3, **(b)** residue 9, **(c)** residue 15, **(d)** residue 16, **(e)** residue 21, and **(f)** residue 22. Sequences containing 8-bromo-guanine (solid line), 8-O-methyl-guanine (dotted line) and 8-amino-guanine (dashed line) modifications are presented. **(g)** CD spectra for multiple-position substitutions are presented for sequences Br-9-22 (solid line), Br-9-Omet-22 (dotted line), and Br-9-Am-22 (dashed line). The unmodified sequence (solid grey line) is again shown as a reference.

Fig. S2. Imino proton NMR spectra for the **(a)** unmodified sequence, as well as modified sequences **(b)** Br-9, **(c)** Omet-9, **(d)** Am-9, and **(e)** Oxo-9 containing a single substitution to *syn* residue 9. The unmodified spectrum is labeled with the residue numbers with circled numbers representing guanines within the modified G9•G3•G21•G17 tetrad and the modified residue 9 shaded grey. Dotted lines identify the chemical shift of imino protons from the unmodified spectra for guanines located outside of the modified tetrad. Black dots indicate the chemical signature of individual imino proton resonances.

Fig. S3. Imino proton NMR spectra for the **(a)** unmodified sequence, as well as modified sequences **(b)** Br-15, **(c)** Omet-15, **(d)** Am-15, and **(e)** Oxo-15 containing a single substitution to *syn* residue 15. The unmodified spectrum is labeled with the residue numbers with circled numbers representing guanines within the modified G15•G23•G5•G11 tetrad and the modified residue 15 shaded grey. Dotted lines identify the chemical shift of imino protons from the unmodified spectra for guanines located outside of the modified tetrad. Black dots indicate the chemical signature of individual imino proton resonances.

Fig. S4. Imino proton NMR spectra for the **(a)** unmodified sequence, as well as modified sequences **(b)** Br-16, **(c)** Omet-16, and **(d)** Am-16 containing a single substitution to *syn* residue 16. The unmodified spectrum is labeled with the residue numbers with circled numbers representing guanines within the modified G16•G22•G4•G10 tetrad and the modified residue 16 shaded grey. Dotted lines identify the chemical shift of imino protons from the unmodified

spectra for guanines located outside of the modified tetrad. Black dots indicate the chemical signature of individual imino proton resonances.

Fig. S5. Imino proton NMR spectra for the **(a)** unmodified sequence, as well as modified sequences **(b)** Br-21, **(c)** Omet-21, and **(d)** Am-21 containing a single substitution to *syn* residue 21. The unmodified spectrum is labeled with the residue numbers with circled numbers representing guanines within the modified G21•G17•G9•G3 tetrad and the modified residue 21 shaded grey. Dotted lines identify the chemical shift of imino protons from the unmodified spectra for guanines located outside of the modified tetrad. Black dots indicate the chemical signature of individual imino proton resonances.

Fig. S6. Imino proton NMR spectra for the **(a)** unmodified sequence, as well as modified sequences **(b)** Br-22, **(c)** Omet-22, and **(d)** Am-22 containing a single substitution to *anti* residue 22. The unmodified spectrum is labeled with the residue numbers with circled numbers representing guanines within the modified G22•G4•G10•G16 tetrad and the modified residue 22 shaded grey. Dotted lines identify the chemical shift of imino protons from the unmodified spectra for guanines located outside of the modified tetrad. Black dots indicate the chemical signature of individual imino proton resonances.

Fig. S7. Imino proton NMR spectra for the **(a)** unmodified sequence, as well as modified sequences **(b)** Br-9-22, **(c)** Br-9-Omet-22, and **(d)** Br-9-Am-22 containing a substitution to *syn* 9 and *anti* residue 22. The unmodified spectrum is labeled with the residue numbers with circled numbers representing guanines within the modified G22•G4•G10•G16 or G9•G3•G21•G17 tetrads and the modified residues 9 and 22 shaded grey. Dotted lines identify the chemical shift of imino protons from the unmodified spectra for guanines located outside of the modified tetrad. Black dots indicate the chemical signature of individual imino proton resonances.

Fig. S8. Normalized melting curves for sequences containing single-position substitutions of **(a)** 8-bromo-guanine, **(b)** 8-O-methyl-guanine, **(c)** 8-amino-guanine and **(d)** 8-oxo-guanine as well as **(e)** multiple-position substitutions: Sequences containing single-position *syn* substitutions (solid line) are shown for residues 3 (circle), 9 (square), 15 (diamond), 16 (downwards triangle),

and 21 (upwards triangle). Sequences containing single-position *anti* substitutions (dotted line) are shown for residue 22 (square). The *unmodified* sequence is shown for reference. (grey dotted line)

Fig. S9. Raw UV absorption data for thermal denaturing experiments: Markers indicate data points from the cooling curve. The heating curve is represented by a solid line. Data for single position substitutions is presented for substitution into **(a)** residue 3, **(b)** residue 9, **(c)** residue 15, **(d)** residue 16, **(e)** residue 21 and **(f)** residue 22 for guanine derivatives 8-bromo-guanine (circle), 8-O-methyl-guanine (square), 8-amino-guanine (diamond) and 8-oxo-guanine (triangle). Thermal denaturing data for **(g)** Multiple-position substitutions and **(h)** the unmodified sequence is also presented.

Fig. S10. Observation of 8-bromo-guanine modification driven change in imino proton chemical shift: **(a)** The NMR imino proton spectrum of the unmodified spectrum is presented as a reference with labeled resonances. The spectra of sequences containing single-position *syn* 8-bromo-guanine substitutions including **(b)** Br-3, **(c)** Br-9, **(d)** Br-15, **(e)** Br-16, **(f)** and Br-21 are presented with accompanying ^{15}N-labeling experiments identifying unambiguously the resonance of the G_δ imino proton. (reference Figure 4). Arrows are used to indicate the magnitude and direction of change in chemical shift for the G_δ imino proton.

Fig. S11. Observation of 8-O-methyl-guanine modification driven change in imino proton chemical shift: **(a)** The NMR imino proton spectrum of the unmodified spectrum is presented as a reference with labeled resonances. The spectra of sequences containing single-position *syn* 8-O-methyl-guanine substitutions including **(b)** Omet-3, **(c)** Omet-9, **(d)** Omet-15, **(e)** Omet-16, **(f)** and Omet-21 are presented with accompanying ^{15}N-labeling experiments identifying unambiguously the resonance of the G_δ imino proton. (reference Figure 4). Arrows are used to indicate the magnitude and direction of change in chemical shift for the G_δ imino proton.

Fig. S12. Observation of 8-amino-guanine modification driven change in imino proton chemical shift: **(a)** The NMR imino proton spectrum of the unmodified spectrum is presented as a reference with labeled resonances. The spectra of sequences containing single-position *syn* 8-

amino-guanine substitutions including **(b)** Am-3, **(c)** Am-9, **(d)** Am-15, **(e)** Am-16, **(f)** and Am-21 are presented with accompanying ^{15}N-labeling experiments identifying unambiguously the resonance of the G_{δ} imino proton. (reference Figure 4). Arrows are used to indicate the magnitude and direction of change in chemical shift for the G_{δ} imino proton.

Fig. S13. Imino and aromatic proton regions of the NMR spectra for the **(a)** unmodified, **(b)** Br-3, **(c)** Br-9, **(d)** Br-15, **(e)** Br-16, **(f)** Br-21, **(g)** Br-22 and **(h)** Br-9-22 sequences.

Fig. S14. Imino and aromatic proton regions of the NMR spectra for the **(a)** unmodified, **(b)** Omet-3, **(c)** Omet-9, **(d)** Omet-15, **(e)** Omet-16, **(f)** Omet-21, **(g)** Omet-22 and **(h)** Br-9-Omet-22 sequences.

Fig. S15. Imino and aromatic proton regions of the NMR spectra for the **(a)** unmodified, **(b)** Am-3, **(c)** Am-9, **(d)** Am-15, **(e)** Am-16, **(f)** Am-21, **(g)** Am-22 and **(h)** Br-9-Am-22 sequences.

Fig. S16. Imino and aromatic proton regions of the NMR spectra for the **(a)** unmodified, **(b)** Oxo-3, **(c)** Oxo-9, **(d)** Oxo-15 sequences.

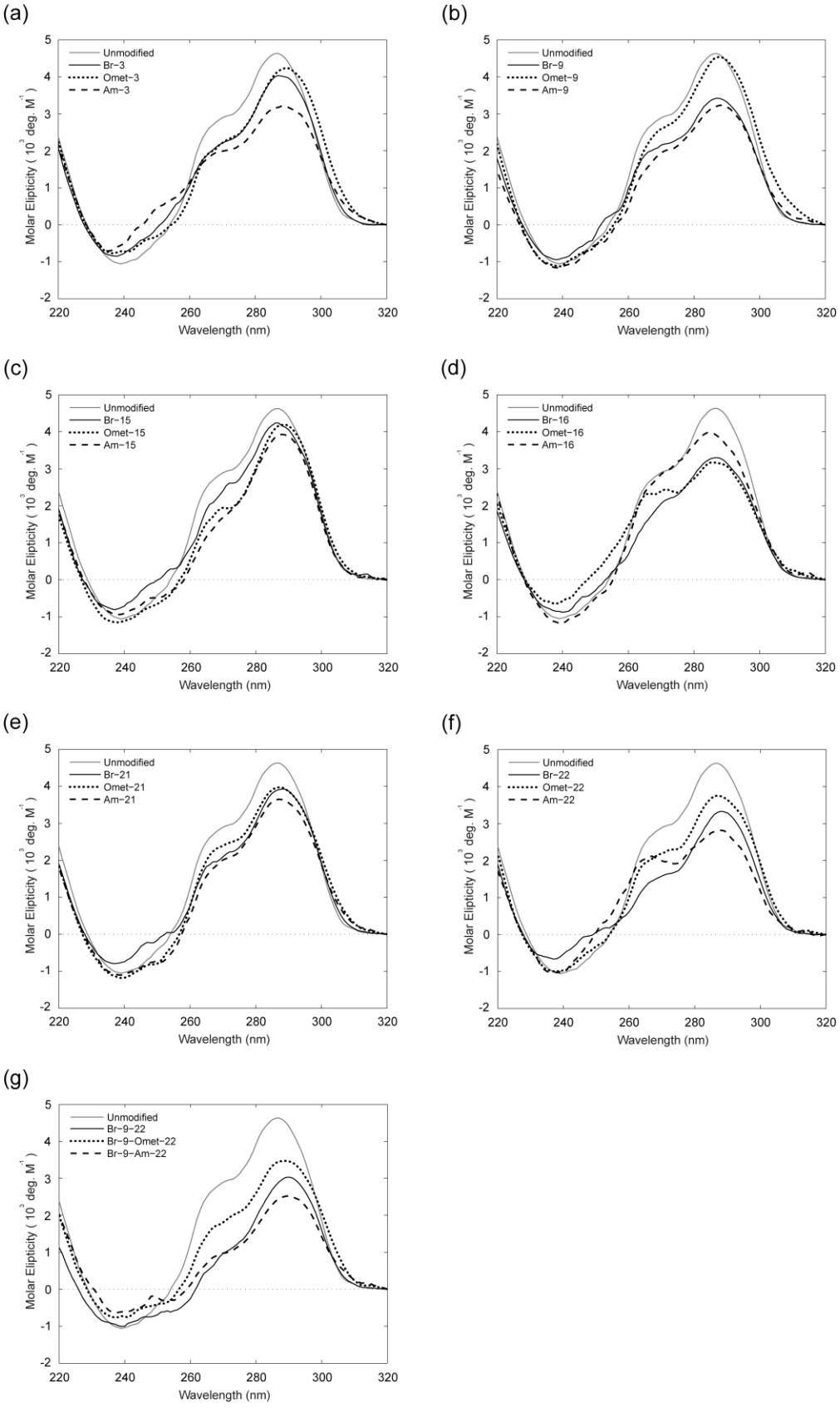
(a)
Unmodified
Br−3
Omet−3
Am−3
(b)
Unmodified
Br−9
Omet−9
Am−9
(c)
Unmodified
Br−15
Omet−15
Am−15
(d)
Unmodified
Br−16
Omet−16
Am−16
(e)
Unmodified
Br−21
Omet−21
Am−21
(f)
Unmodified
Br−22
Omet−22
Am−22
(g)
Unmodified
Br−9−22
Br−9−Omet−22
Br−9−Am−22
Molar Elipticity (10^3 deg. M^-1)
Wavelength (nm)

Figure S1

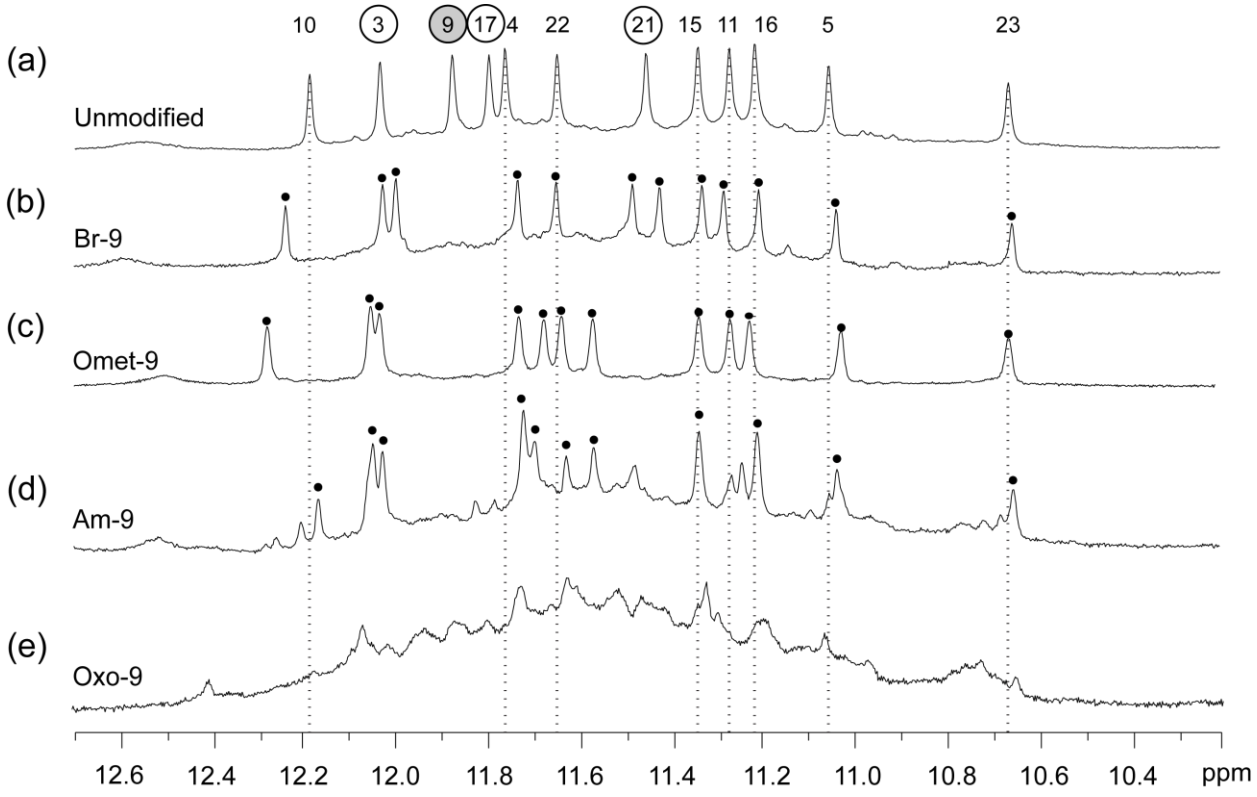
10
3
9
17
4
22
21
15
11
16
5
23
(a)
Unmodified
(b)
Br-9
(c)
Omet-9
(d)
Am-9
(e)
Oxo-9
12.6
12.4
12.2
12.0
11.8
11.6
11.4
11.2
11.0
10.8
10.6
10.4
ppm

Figure S2

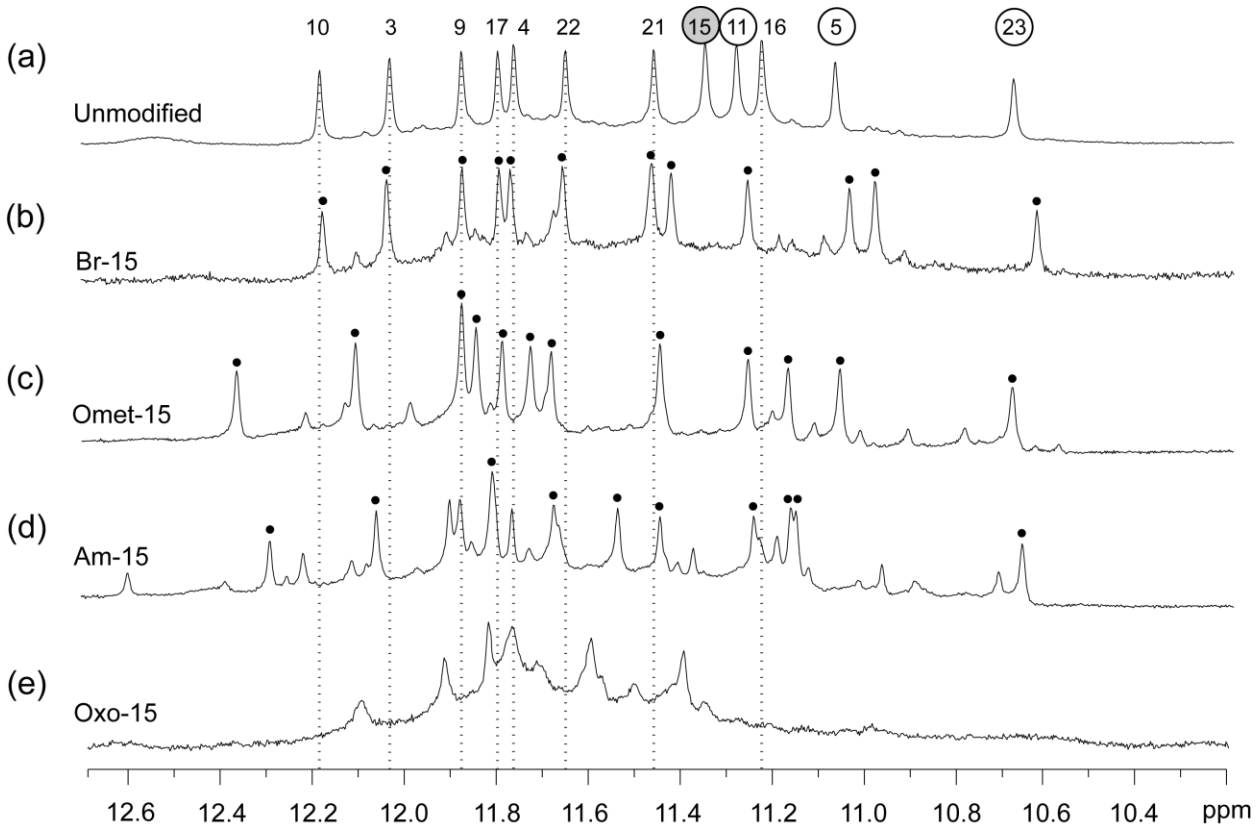
10
3
9
17
4
22
21
15
11
16
5
23
(a)
Unmodified
(b)
Br-15
(c)
Omet-15
(d)
Am-15
(e)
Oxo-15
12.6
12.4
12.2
12.0
11.8
11.6
11.4
11.2
11.0
10.8
10.6
10.4
ppm

Figure S3

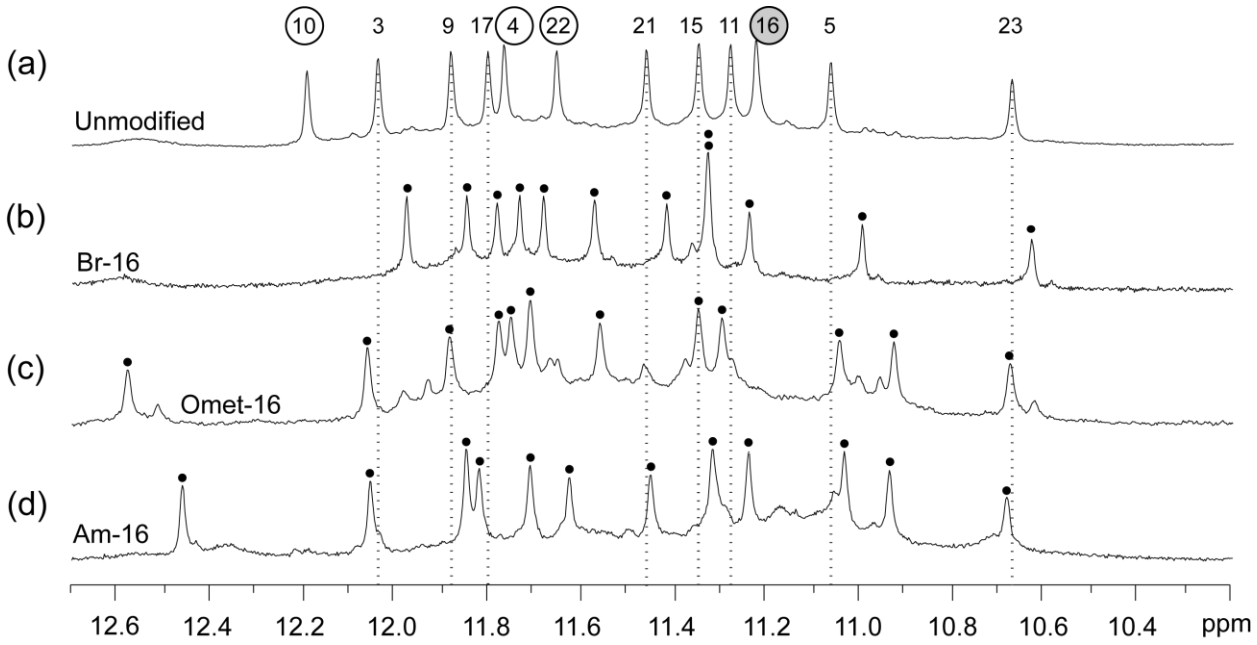
10
3
9
17
4
22
21
15
11
16
5
23
(a)
Unmodified
(b)
Br-16
(c)
Omet-16
(d)
Am-16
12.6
12.4
12.2
12.0
11.8
11.6
11.4
11.2
11.0
10.8
10.6
10.4
ppm

Figure S4

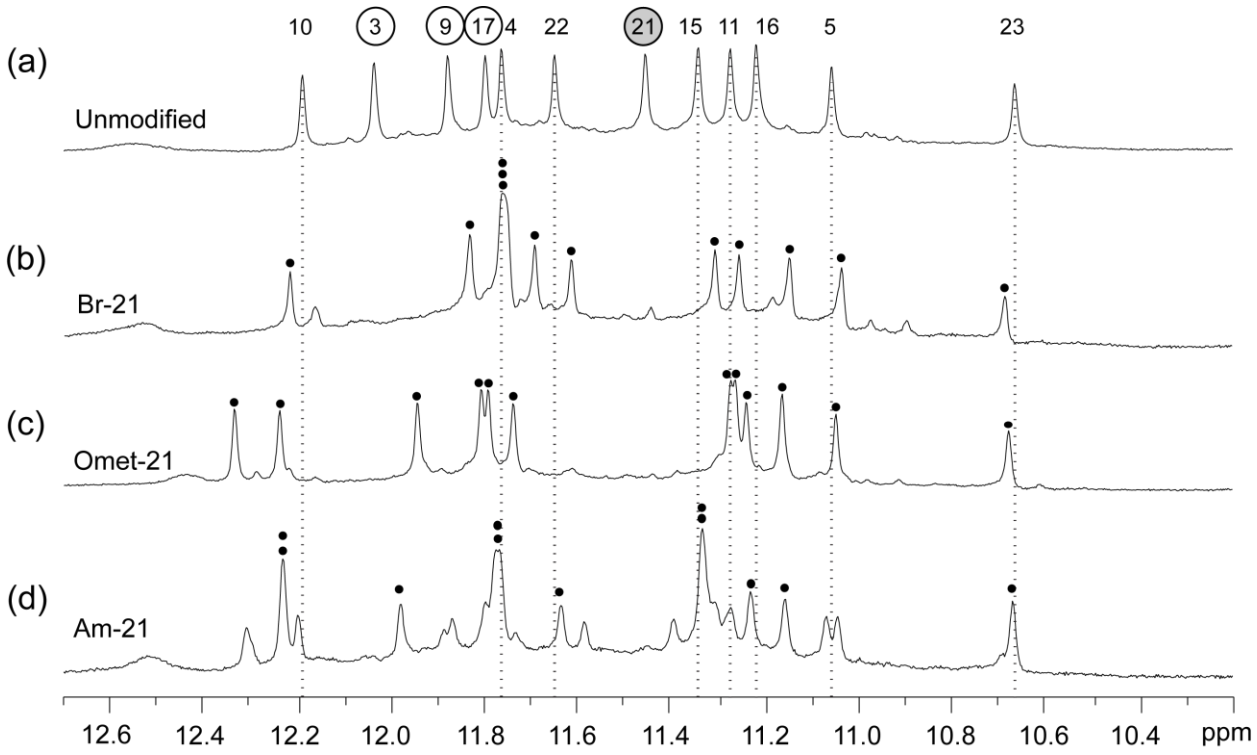
10
3
9
17
4
22
21
15
11
16
5
23
(a)
Unmodified
(b)
Br-21
(c)
Omet-21
(d)
Am-21
12.6
12.4
12.2
12.0
11.8
11.6
11.4
11.2
11.0
10.8
10.6
10.4
ppm

Figure S5

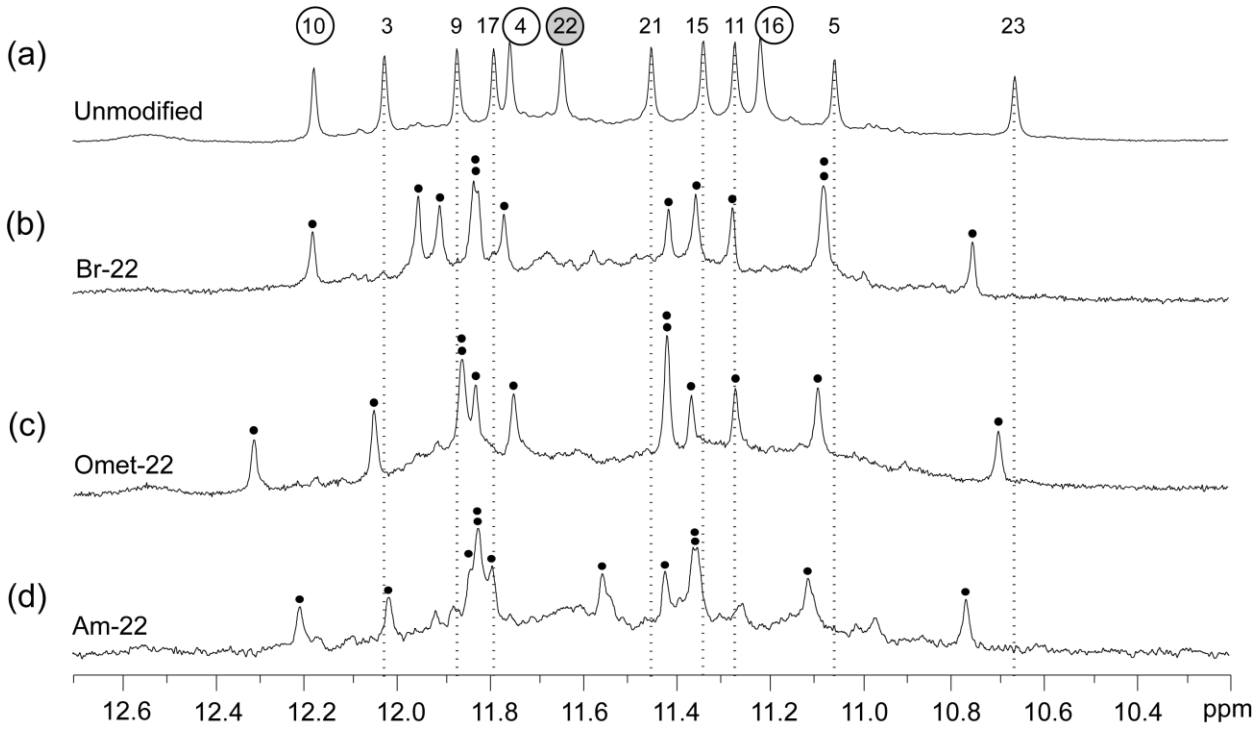
(a)
Unmodified
(b)
Br-22
(c)
Omet-22
(d)
Am-22
10
3
9
17
4
22
21
15
11
16
5
23
12.6
12.4
12.2
12.0
11.8
11.6
11.4
11.2
11.0
10.8
10.6
10.4
ppm

Figure S6

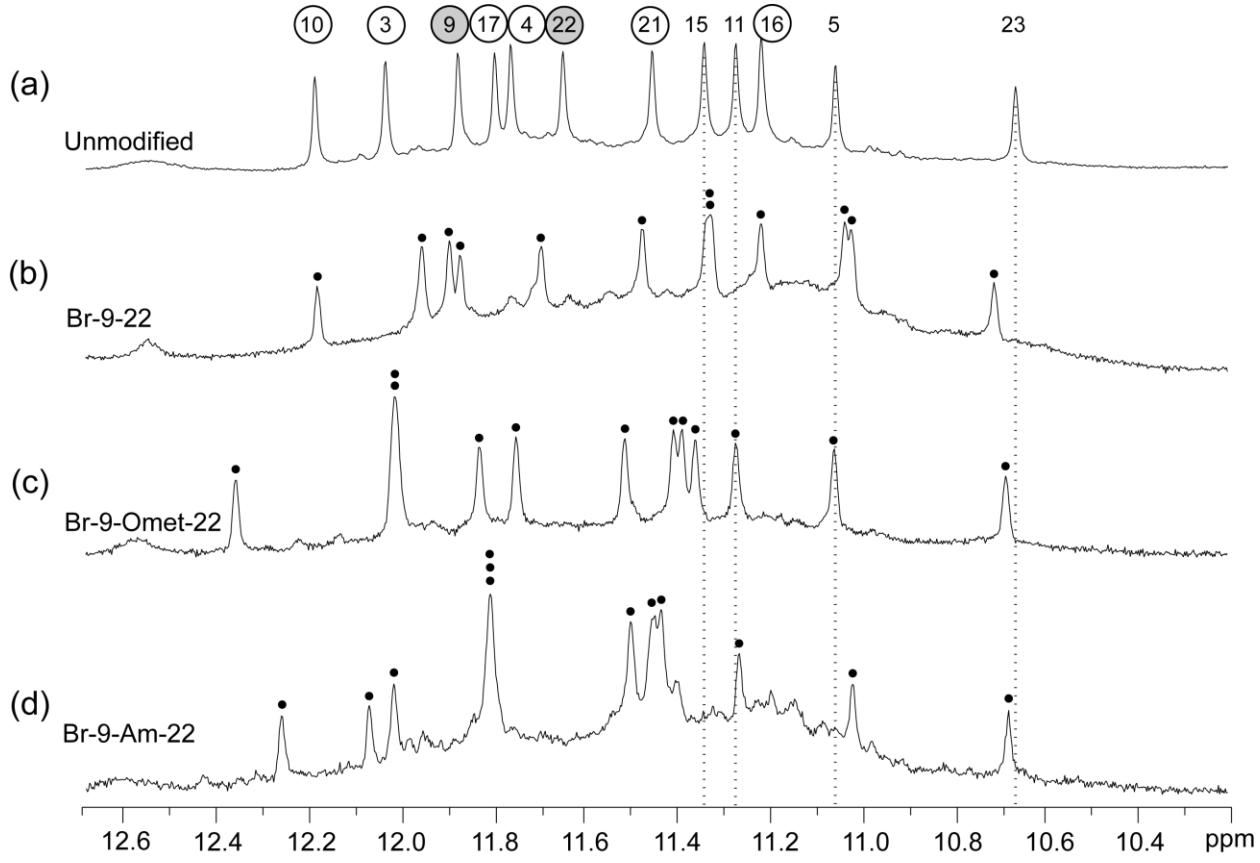
10
3
9
17
4
22
21
15
11
16
5
23
(a)
Unmodified
(b)
Br-9-22
(c)
Br-9-Omet-22
(d)
Br-9-Am-22
12.6
12.4
12.2
12.0
11.8
11.6
11.4
11.2
11.0
10.8
10.6
10.4
ppm

Figure S7

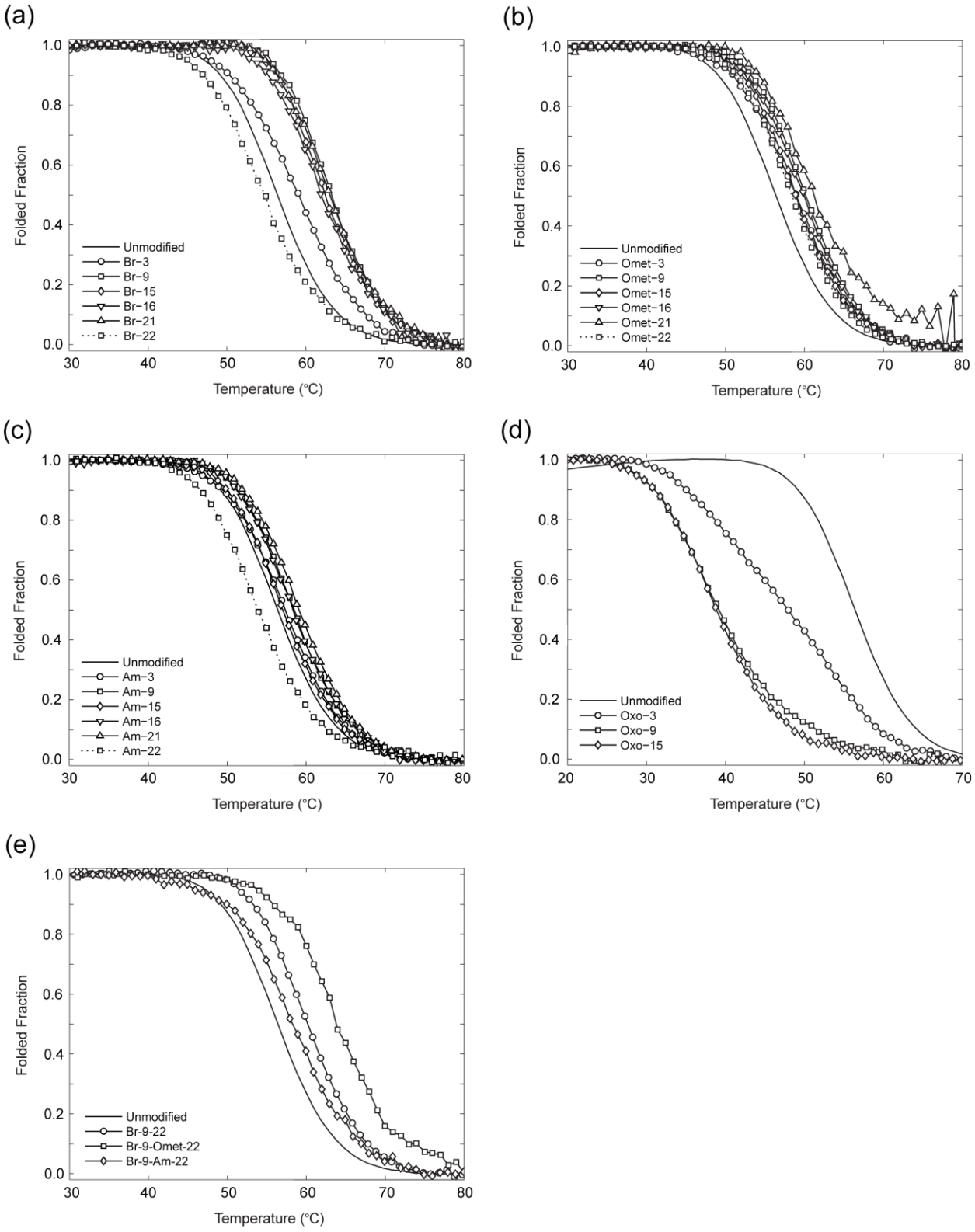
(a)
Folded Fraction
Temperature (°C)
Unmodified
Br−3
Br−9
Br−15
Br−16
Br−21
Br−22
(b)
Folded Fraction
Temperature (°C)
Unmodified
Omet−3
Omet−9
Omet−15
Omet−16
Omet−21
Omet−22
(c)
Folded Fraction
Temperature (°C)
Unmodified
Am−3
Am−9
Am−15
Am−16
Am−21
Am−22
(d)
Folded Fraction
Temperature (°C)
Unmodified
Oxo−3
Oxo−9
Oxo−15
(e)
Folded Fraction
Temperature (°C)
Unmodified
Br-9-22
Br-9-Omet-22
Br-9-Am-22

Figure S8

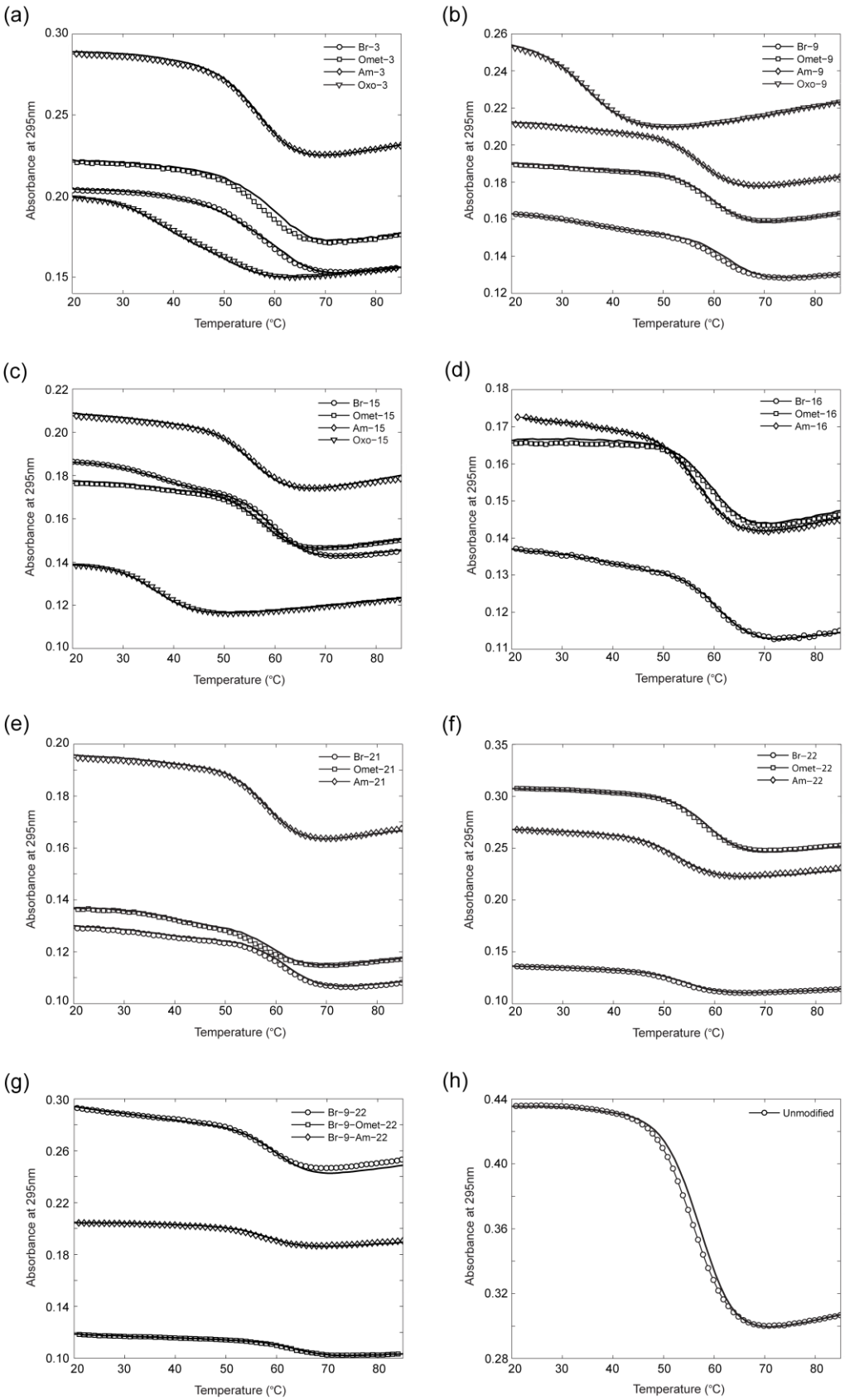
(a)
Br−3
Omet−3
Am−3
Oxo−3
Absorbance at 295nm
Temperature (°C)
(b)
Br−9
Omet−9
Am−9
Oxo−9
Absorbance at 295nm
Temperature (°C)
(c)
Br−15
Omet−15
Am−15
Oxo−15
Absorbance at 295nm
Temperature (°C)
(d)
Br−16
Omet−16
Am−16
Absorbance at 295nm
Temperature (°C)
(e)
Br−21
Omet−21
Am−21
Absorbance at 295nm
Temperature (°C)
(f)
Br−22
Omet−22
Am−22
Absorbance at 295nm
Temperature (°C)
(g)
Br−9−22
Br−9−Omet−22
Br−9−Am−22
Absorbance at 295nm
Temperature (°C)
(h)
Unmodified
Absorbance at 295nm
Temperature (°C)

Figure S9

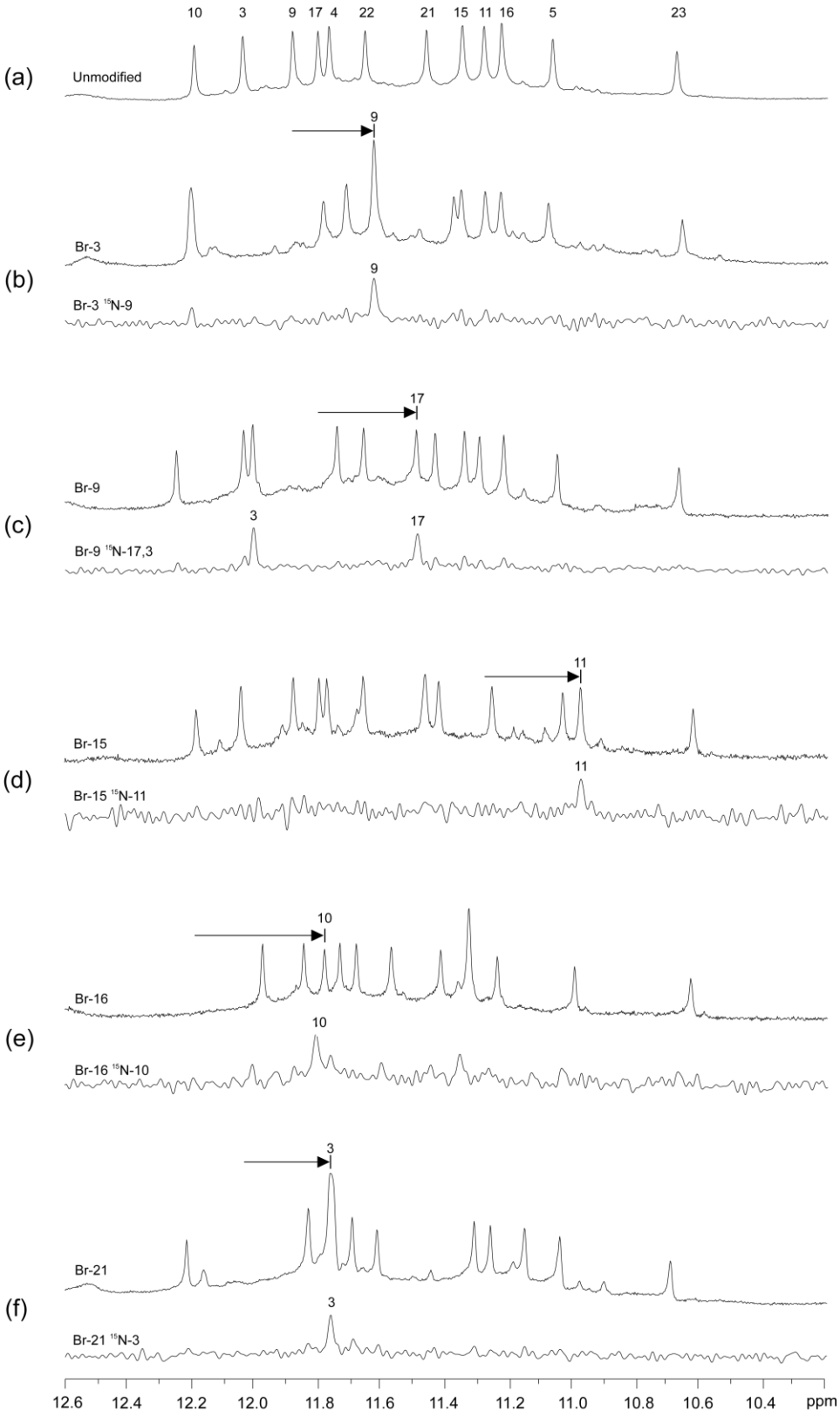
(a)
Unmodified
10
3
9
17
4
22
21
15
11
16
5
23
(b)
Br-3
Br-3 15N-9
9
(c)
Br-9
Br-9 15N-17,3
17
3
17
(d)
Br-15
Br-15 15N-11
11
11
(e)
Br-16
Br-16 15N-10
10
10
(f)
Br-21
Br-21 15N-3
3
3
12.6
12.4
12.2
12.0
11.8
11.6
11.4
11.2
11.0
10.8
10.6
10.4
ppm

Figure S10

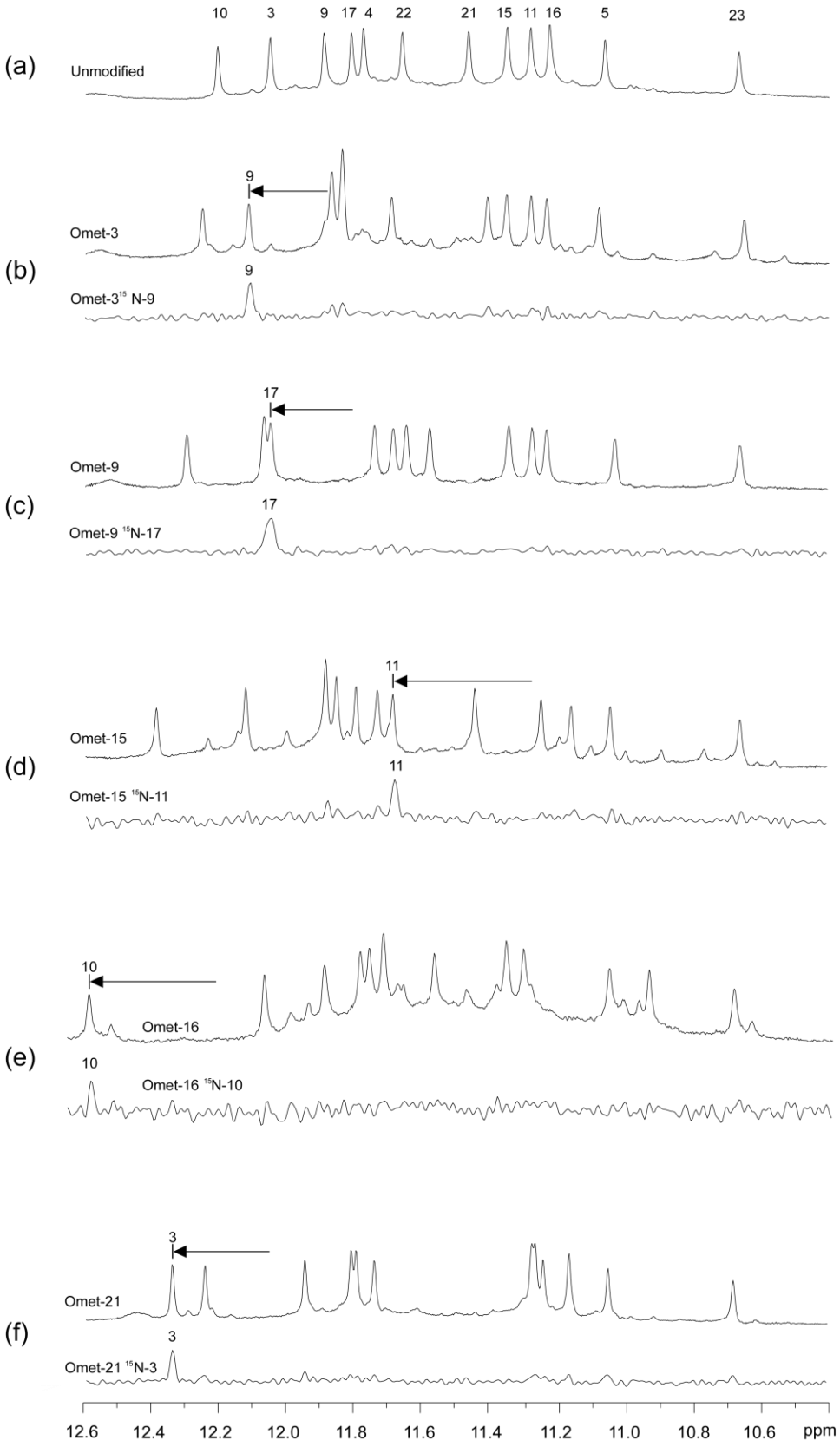
(a)
Unmodified
10
3
9
17
4
22
21
15
11
16
5
23
(b)
Omet-3
9
Omet-3 15 N-9
9
(c)
Omet-9
17
Omet-9 15N-17
17
(d)
Omet-15
11
Omet-15 15N-11
11
(e)
10
Omet-16
Omet-16 15N-10
10
(f)
Omet-21
3
Omet-21 15N-3
3
12.6
12.4
12.2
12.0
11.8
11.6
11.4
11.2
11.0
10.8
10.6
ppm

Figure S11

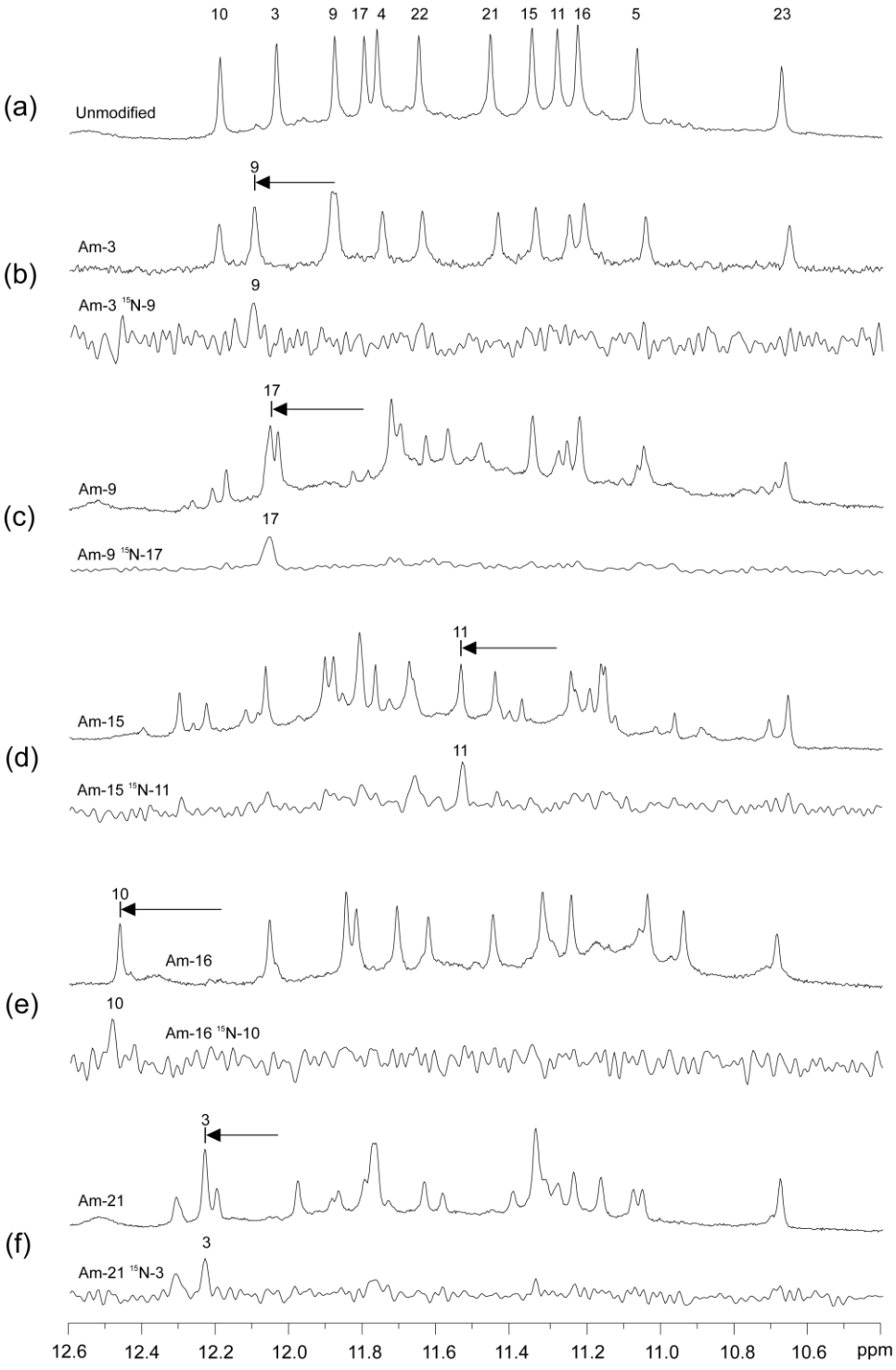
10 3 9 17 4 22 21 15 11 16 5 23
(a)
Unmodified
9
Am-3
(b)
9
Am-3 15N-9
17
Am-9
(c)
17
Am-9 15N-17
11
Am-15
(d)
11
Am-15 15N-11
10
Am-16
(e)
10
Am-16 15N-10
3
Am-21
(f)
3
Am-21 15N-3
12.6 12.4 12.2 12.0 11.8 11.6 11.4 11.2 11.0 10.8 10.6 ppm

Figure S12

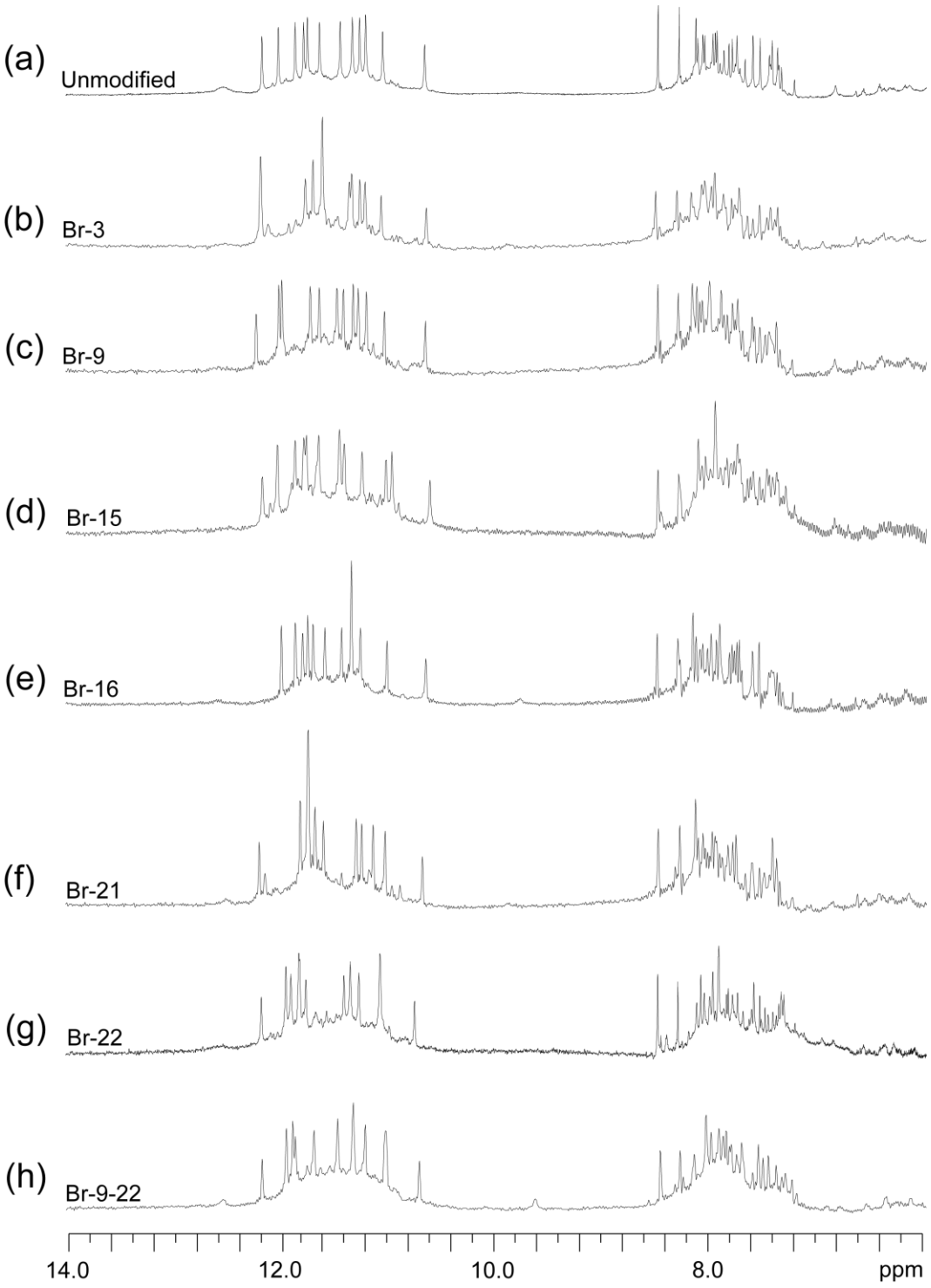
(a) Unmodified
(b) Br-3
(c) Br-9
(d) Br-15
(e) Br-16
(f) Br-21
(g) Br-22
(h) Br-9-22
14.0
12.0
10.0
8.0
ppm

Figure S13

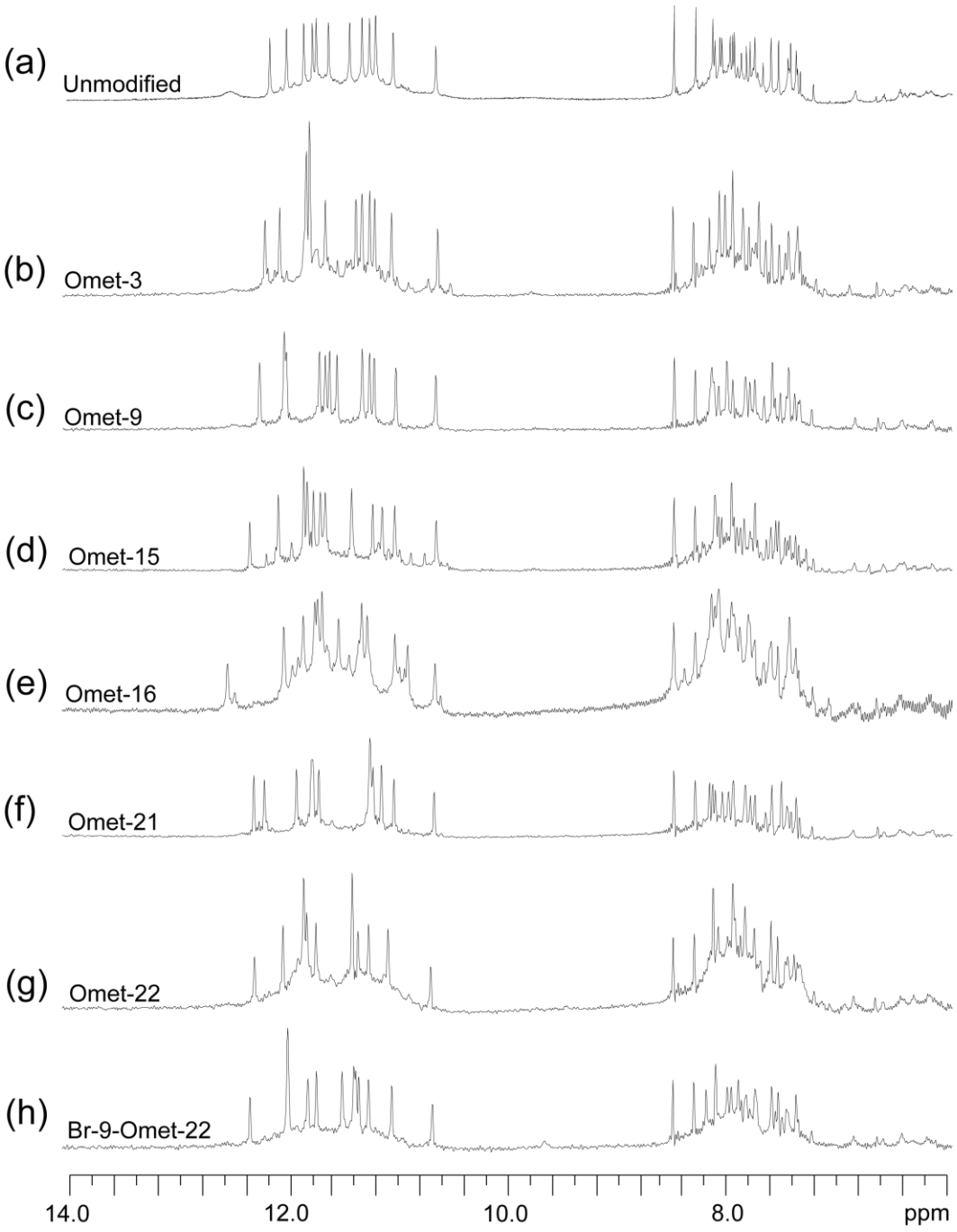
(a) Unmodified
(b) Omet-3
(c) Omet-9
(d) Omet-15
(e) Omet-16
(f) Omet-21
(g) Omet-22
(h) Br-9-Omet-22
14.0
12.0
10.0
8.0
ppm

Figure S14

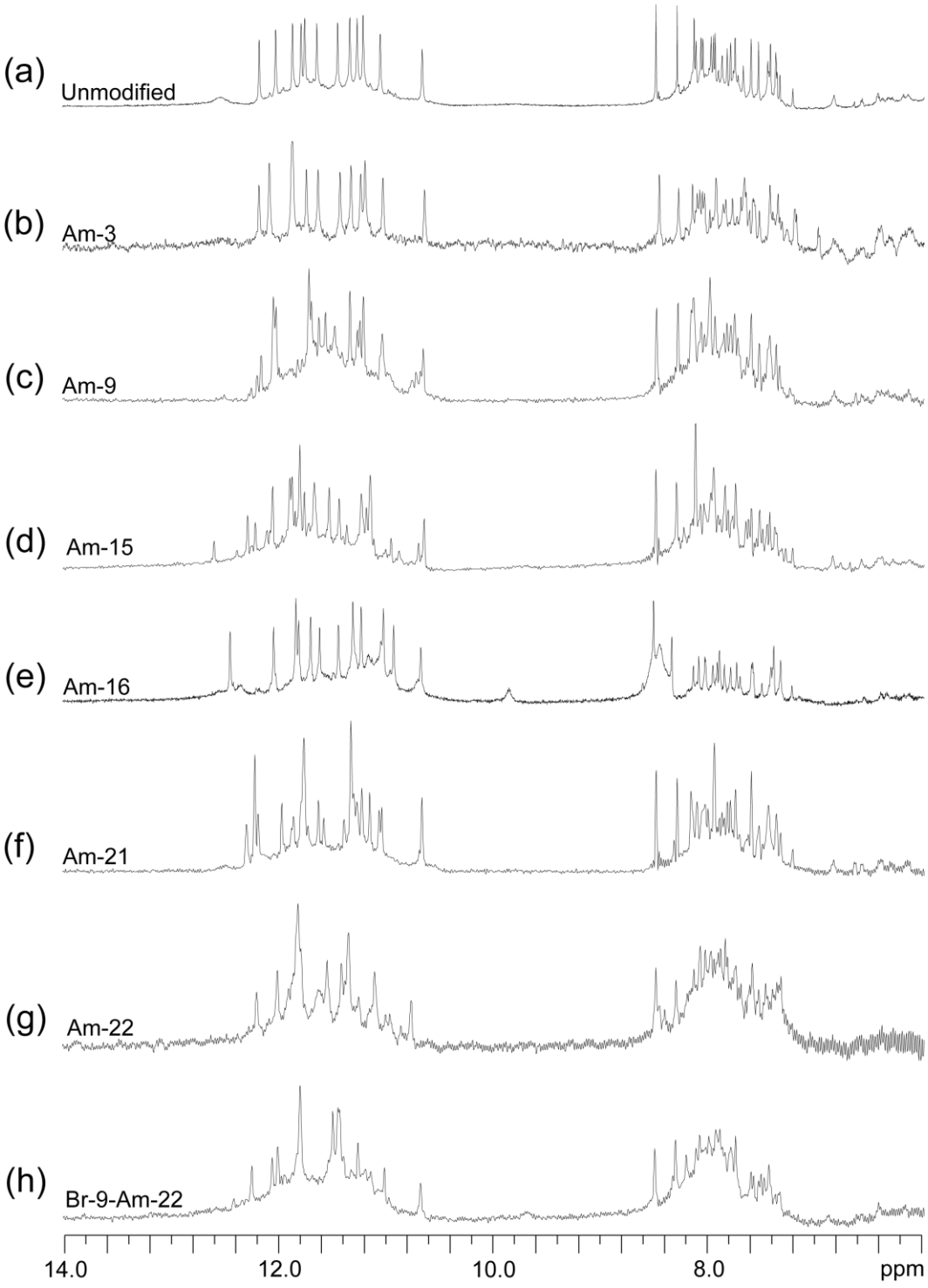
(a) Unmodified
(b) Am-3
(c) Am-9
(d) Am-15
(e) Am-16
(f) Am-21
(g) Am-22
(h) Br-9-Am-22
14.0
12.0
10.0
8.0
ppm

Figure S15

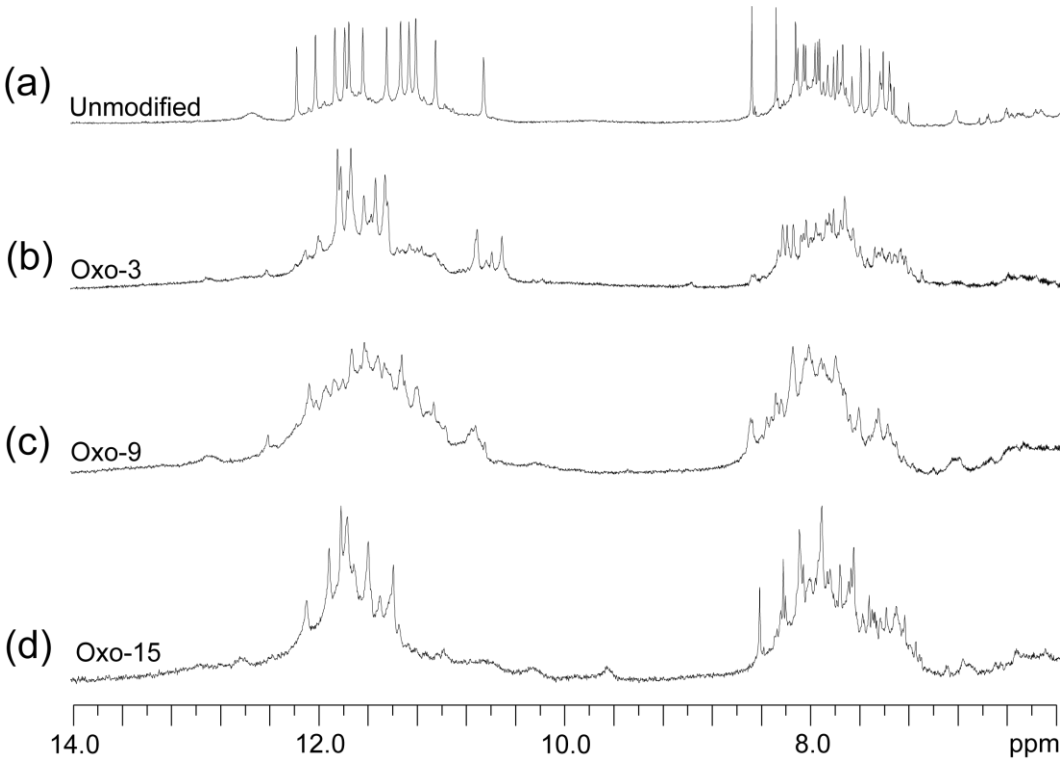

Figure S16